

# Experimental Quantification of Implementation Penalties from Laser Phase Noise for Ultra-High-Order QAM Signals

Xi Chen, Junho Cho, and Di Che

Nokia Bell Labs, Holmdel, NJ, USA, [xi.v.chen@nokia-bell-labs.com](mailto:xi.v.chen@nokia-bell-labs.com)

**Abstract** We experimentally characterize ultra-high order QAM (256-, 1024-, and 4096- QAM) signals' tolerance to laser phase noise. The studied phase noise covers a wide range from 200 Hz to 10 MHz.

## Introduction

Several high spectral efficiency (SE) systems with ultra-high-order quadrature amplitude modulation (QAM) have been demonstrated over the past few years<sup>[1-7]</sup>. For instance, Ref. 1 used 4096-QAM to achieve an SE of 15.8 bit/s/Hz. In Ref. 7, 16384-QAM was used with probabilistic shaping (PS) to reach an information rate (IR) of 22.3 bit/symbol/2-pol. Generating and detecting ultra-high order QAM signals is challenging. The implementation penalties can be induced by quantization noise<sup>[8]</sup>, or in-phase/quadrature (I/Q) imbalance from optical transmitters and receivers<sup>[7]</sup>. Besides these, laser phase noise is also one of the main sources of the penalties. Understanding the phase noise tolerance for high order QAM constellations is important<sup>[9, 10]</sup>. However, there is no systematic measurement on the tolerance for QAM orders higher than 256. Experiments where 1024 QAM and higher formats are adopted tend to use very low linewidth fiber lasers. For instance, the 4096-QAM demonstration uses lasers with linewidth < 100 Hz<sup>[2]</sup>, and experiment in Ref.1 uses an optical phase locking loop circuit to reduce the phase noise as much as possible.

In this paper, we characterize the laser phase noise tolerance of 256-, 1024- and 4096-QAM constellations. We emulate a wide range of laser linewidths via adding phase noise with I/Q modulation<sup>[11,12]</sup>. In an experimental system with 4% pilot aided phase compensation, our results show that 256-, 1024-, and 4096-QAM at 10 GBaud can tolerate up to 100 kHz, 15 kHz, and 2 kHz laser linewidths, respectively, at an optical SNR (OSNR) penalty of 1 dB.

## Experimental setup

The experimental setup for characterizing the phase noise tolerance is shown in Fig. 1. The transmitter consists of a laser with a linewidth of ~100 Hz operating at 1550.1192 nm<sup>[13]</sup>, and a LiNbO<sub>3</sub> single-polarization I/Q Mach-Zehnder modulator (MZM) with a 3-dB bandwidth of 35 GHz and a  $V_{\pi}$  of ~ 3.5 V. The modulator uses a laser input power of 19 dBm and is driven by 28-nm CMOS digital-to-analog converters (DACs)

with 8-bit nominal resolution and a 3-dB bandwidth of ~18 GHz. The 10-GBaud baseband QAM signals are digitally up-shifted by 6 dB and loaded on two DACs for I and Q signal components, such that the modulator produces single-side band (SSB) signals with the optical spectrum shown in Fig. 1. This eliminates the penalties from the frequency-dependent transmitter I/Q imbalance<sup>[7]</sup> and hence allows to better observe the performance degradation due to laser phase noise. The DACs are operated at 88 GSa/s and their differential outputs are converted to a single-ended signal via RF baluns. The signal driving the modulator has a peak-to-

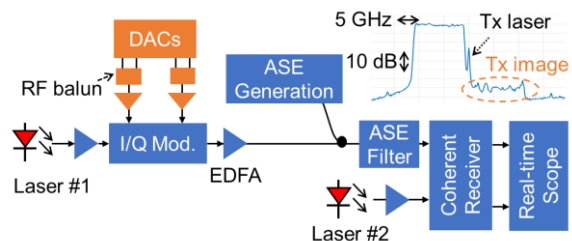


Fig. 1 Experimental setup for characterizing phase noise tolerance. The inset show the optical spectrum.

peak voltage of ~1.3 V. The modulated light is amplified by an erbium-doped fiber amplifier (EDFA), with an output optical signal-to-noise ratio (OSNR) of 46.7 dB. The received signal is filtered by a bandpass amplified spontaneous emission (ASE) filter with 100-GHz pass bandwidth. Detection is done by a coherent receiver that consists of two balanced detectors (BPDs, 3-dB bandwidth of 45 GHz) and two analog-to-digital converters (ADCs, two channels of a real-time oscilloscope operating at 256 GSa/s with an analog bandwidth of 103 GHz and a nominal resolution of 10 bits). The free-running local oscillator (LO, laser #2 in Fig. 1) has a linewidth of ~100 Hz and operates at 1550.1214 nm (275 MHz away from laser #1). In principle, the SSB signal can be received by a standard heterodyne coherent receiver with only one BPD and one ADC. However, we choose to detect in-phase and quadrature components of the optical field using two BPDs, to avoid the *noise folding* problem (3-dB OSNR penalty compared to intradyne structures) inherent to the heterodyne

structures. In this way, we reduce the implementation penalty and better observe the impact of phase noise. As our signal is single polarization, to keep the definition of OSNR consistent with dual-polarization systems, all the OSNRs in this paper are the OSNRs measured by an optical spectrum analyzer (OSA) plus 3 dB, as the OSA measures noise power at both polarizations. We change the OSNR via a noise loading stage as shown in Fig. 1.

### Digital signal processing and phase noise estimation

We study three ultra-high-order QAM formats: 256-, 1024-, and 4096- QAM. All the constellation points are uniformly distributed. Comparison of phase noise tolerance between uniform QAM and PS-QAM is beyond the scope of this paper but can be found in Ref.14. To study the laser phase noise systemically, we emulate a wide range of laser linewidths by digitally adding phase noise to high-order QAM waveforms at the transmitter as

$$s'(t) = s(t) \cdot e^{j\varphi(t)}, \quad (1)$$

where  $s'(t)$  and  $s(t)$  are the digital waveforms at time  $t$  with and without the digitally added phase noise  $\varphi(t)$ , respectively. Here, the phase noise is modelled by a Wiener process as [11,12]

$$\varphi(t) = n_t \sqrt{2\pi\Delta t \Delta f} + \varphi(t - \Delta t), \quad (2)$$

where  $n_t$  is Gaussian noise with zero mean and unit variance,  $\Delta f$  is the targeted digital laser linewidth, and  $\Delta t$  is the sampling time step. Note that in a back-to-back system without dispersive elements in the channel, adding phase noise to the transmitter laser has the same impact as adding it to the receiver laser. In the presence of fiber dispersion, one of the laser linewidths (transmitter or receiver) can be enhanced, and this is a different type of degradation called equalization enhanced phase noise (EEN). The EEN is not in the scope of this paper and has been quantitatively analyzed in Ref.15.

As shown in Fig. 2(a), at the transmitter, after generating QAM signals, root-raised cosine (RRC) pulse shaping (with a roll-off factor of 0.01), waveform up-sampling, and frequency up-shifting are performed. After that, phase noise is added to the waveform according to Eqs. (1) and (2). The waveform is then quantized and loaded to DACs. Our transmitter and receiver lasers each have a linewidth of 100 Hz, and therefore 200 Hz of hardware laser linewidth is added on top of the digitally emulated laser linewidth. As illustrated in Fig. 2 (b), the receiver DSP consists of frequency offset compensation, frame synchronization, and 2-sample/symbol least

mean square (LMS)-based complex-valued channel equalization. The equalizer has 421 taps and uses  $\sim 8,000$  training symbol for pre-convergence. After the equalizer, symbol decision is done and normalized generalized mutual information (NGMI) is calculated. We use a rate-0.8 (25%-overhead) binary spatially-coupled low-density parity-check (SC-LDPC) code (SC Code B of Ref. 16), which does not have an error floor until at a post-FEC BER  $< 10^{-15}$ . It has an NGMI threshold of  $NGMI^* = 0.861$ . The waveform loaded to DACs has a time duration of 2.97  $\mu$ s. For each tested format, about 1 million symbols are used for NGMI calculation.

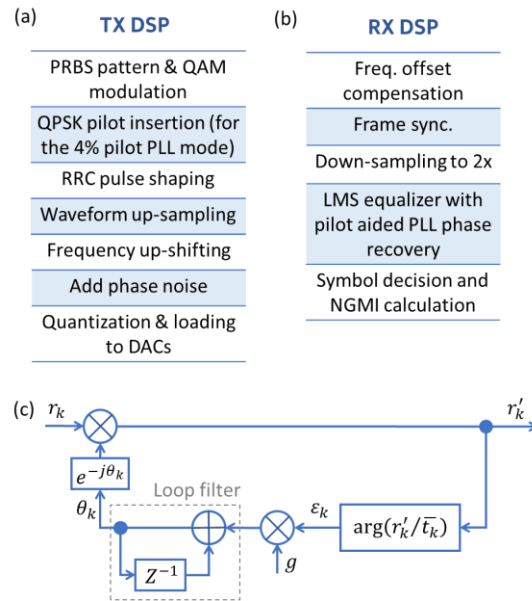


Fig. 2 Digital signal processing procedures at (a) transmitter and (b) receiver; (c) block diagram for the PLL-based phase estimation.

For phase noise compensation at the receiver, we use a pilot-based digital phase locked loop (PLL) [10, 17, 20]. Other known phase noise compensation methods include the  $M^{\text{th}}$ -power algorithm [18] and blind phase search (BPS) [9]. However, they are not chosen in this paper since the  $M^{\text{th}}$  power algorithm cannot be applied to QAM orders higher than 16, and the implementation complexity of the BPS algorithm is too high especially for ultra-high-order QAM. Our digital PLL is a first-order PLL and is embedded in the LMS equalizer. The block diagram of the PLL is shown in Fig. 2(c). The received symbol  $r_k$  is compared with the pilot symbol  $\bar{r}_k$  to get the phase error  $\epsilon_k$ . Then the phase error is multiplied by a weighting parameter  $g$ , and fed into a loop filter for phase tracking. Finally, the output phase  $\theta_k$  is applied to recover the phase. We use the digital PLL in two different modes: 100%-pilot and 4%-pilot modes. In the 100%-pilot mode, the phase errors are

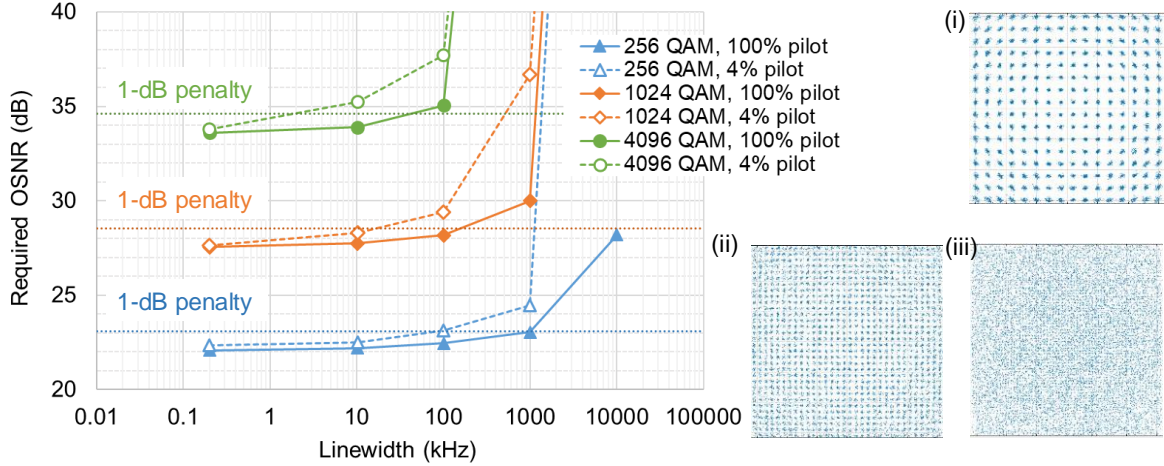


Fig. 3 Required OSNR for the 10-GBaud signals at different linewidths. Insets show constellations of (i) 256 QAM; (ii) 1024 QAM; and (iii) 4096 QAM at the highest available OSNR (46.7 dB) and at each format's highest tolerated linewidth with 4% pilot aided phase estimation.

always calculated relative to the exact transmitted high-order QAM symbols. In this case, there is one symbol delay in the PLL feedback loop. This mode is not practical but is used to see the limit of the underlying pilot-based PLL method. For the 4%-pilot mode that represents a practical scenario, one QPSK symbol is added as the pilot after every 24 high-order QAM symbols, and the PLL feedback delay is 25 symbols. The phase compensation for the data symbols between the two pilots use phase values that are linearly interpolated from the two adjacent pilot symbols. Note the parallelization delay in the application-specific integrated circuit (ASIC) is not considered as it can be avoided by using superscalar PLL structure as pointed out in Ref.19 and Ref.20.

### Results and discussion

For each modulation format, we add four different digital linewidths of 10 kHz, 100 kHz, 1 MHz, and 10 MHz, and measure the NGMI as a function of OSNR. We determine the required OSNR at 25% overhead FEC threshold (NGMI\*=0.861). The required OSNRs measured for the 256-, 1024-, and 4096-QAM signals at 10 GBaud are shown in Fig. 3. Typically, the laser phase noise is considered as tolerable if the laser linewidth increases the required OSNR by less than 1 dB compared to an ideal system with zero phase noise<sup>[9,10]</sup>. Our simulations show that 200-Hz linewidth incurs a negligible OSNR penalty (< 0.03 dB), hence in the experiment we estimate the OSNR penalty relative to the system operated in the 100%-pilot mode with the 200-Hz physical laser linewidth and zero digital linewidth. The required OSNR values at 1-dB penalty are drawn as dashed horizontal lines in Fig. 3. From the figure, we can see that in the 100%-pilot mode,

256-, 1024-, and 4096-QAM constellations can tolerate up to 1 MHz, 150 kHz, and 40 kHz linewidth, respectively. In the 4%-pilot mode, they can tolerate 100 kHz, 15 kHz, and 2 kHz, respectively. The insets (i)-(iii) in Fig. 3 show the recovered 256-, 1024-, and 4096- QAM constellations in the 4%-pilot mode with linewidths of 100 kHz, 10 kHz, and 100 Hz, at OSNR of 46.7 dB.

Figure 4 shows the required  $\Delta f \cdot T_{sym}$  (where  $T_{sym}$  is the symbol duration) for the three formats. At the 1-dB OSNR penalty, 1024-QAM in the 4%-pilot mode requires  $\Delta f \cdot T_{sym}$  of  $1.5 \times 10^{-6}$ , which implies, e.g., a 30-GBaud 1024-QAM signal can tolerate 45-kHz linewidth, and a 100-GBaud 1024-QAM signal can tolerate 150-kHz linewidth.

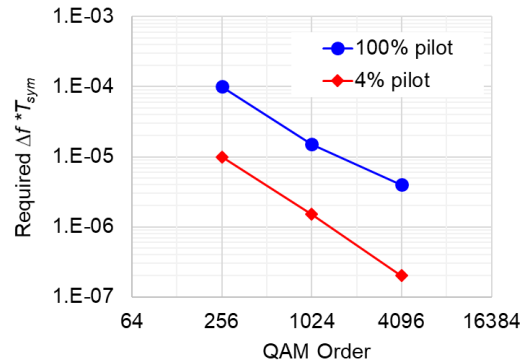


Fig. 4 Required  $\Delta f \cdot T_{sym}$  for the 256-, 1024-, and 4096- QAM signals.

### Conclusions

We measure phase noise tolerance of 256-, 1024-, and 4096- QAM signals. Our results show that 256-, 1024-, and 4096-QAM at 10 GBaud can tolerate up to 100 kHz, 15 kHz, and 2 kHz linewidths to meet a 25%-overhead FEC threshold with up to 1 dB of the OSNR penalty.

## References

- [1] M. Terayama, *et al.*, "4096 QAM (72 Gbit/s) single-carrier coherent optical transmission with a potential SE of 15.8 bit/s/Hz in all-Raman amplified 160 km fiber link," OFC'2018, paper Th1F.2.
- [2] S. Olsson, *et al.*, "Record-high 17.3-bit/s/Hz spectral efficiency transmission over 50 km using PS-PDM 4096-QAM," OFC'2018, paper Th4C.5.
- [3] X. Chen, *et al.*, "Transmission of 30-GBd polarization-multiplexed probabilistically shaped 4096-QAM over 50.9-km SSMF", Optics Express **27**: 29916-29923 (2019).
- [4] Y. Wang, *et al.*, "Single-channel 200 Gbit/s, 10 Gsymbol/s-1024 QAM injection-locked coherent transmission over 160 km with a pilot-assisted adaptive equalizer." Optics Express **26**, 17015-17024 (2018).
- [5] S. Beppu, *et al.*, "2048 QAM (66 Gbit/s) single-carrier coherent optical transmission over 150 km with a potential SE of 15.3 bit/s/Hz." Optics express **23**: 4960-4969 (2015).
- [6] Y. Koizumi, *et al.*, "1024 QAM (60 Gbit/s) single-carrier coherent optical transmission over 150 km." Optics Express **20**: 12508-12514 (2012).
- [7] X. Chen, *et al.* "16384-QAM transmission at 10 GBd over 25-km SSMF using polarization-multiplexed probabilistic constellation shaping", ECOC'2019, paper PD.3.3.
- [8] X. Chen, *et al.* "Experimental quantification of implementation penalties from limited ADC resolution for Nyquist shaped higher-order QAM." OFC'2016, paper W4A.3.
- [9] T. Pfau, *et al.*, "Hardware-efficient coherent digital receiver concept with feedforward carrier recovery for M-QAM constellations." Journal of Lightwave Technology **27**: 989-999 (2009).
- [10] E. Ip, *et al.*, "Coherent detection in optical fiber systems." Optics Express **16**: 753-791 (2008).
- [11] X. Chen, *et al.*, "Characterization and monitoring of laser linewidths in coherent systems." Journal of Lightwave Technology **29**: 2533-2537 (2011).
- [12] Z. Zan, *et al.*, "Experimental demonstration of a flexible and stable semiconductor laser linewidth emulator," Opt. Express **18**, 13880-13885 (2010).
- [13] <https://www.nktphotonics.com/lasers-fibers/product/koheras-basik-low-noise-single-frequency-oem-laser-modules/>
- [14] T. Sasai, *et al.*, "Laser phase noise tolerance of uniform and probabilistically shaped QAM signals for high spectral efficiency systems." Journal of Lightwave Technology **38**: 439-446 (2020).
- [15] W. Shieh, *et al.*, "Equalization-enhanced phase noise for coherent-detection systems using electronic digital signal processing," Optics Express **16**, 15718-15727 (2008).
- [16] A. Alvarado, *et al.* "Replacing the soft-decision FEC limit paradigm in the design of optical communication systems." Journal of Lightwave Technology **33**: 4338-4352 (2015).
- [17] X. Zhou, *et al.*, "Low-complexity, blind phase recovery for coherent receivers using QAM modulation." In OFC'2011, paper OMJ3.
- [18] A. J. Viterbi, *et al.*, "Nonlinear estimation of PSK-modulated carrier phase with application to burst digital transmission", IEEE Transactions on Information Theory **29**, 543-551 (1983).
- [19] K. Piyawanno, *et al.*, "Low complexity carrier recovery for coherent QAM using superscalar parallelization," ECOC'2010, paper We.7.A.3.
- [20] Q. Zhuge, *et al.*, "Pilot-aided carrier phase recovery for M-QAM using superscalar parallelization based PLL," Optics Express **20**: 19599-19609 (2012).